



Electrical conductivity of wadsleyite at high temperatures and high pressures

Lidong Dai^{a,b}, Shun-ichiro Karato^{b,*}

^a Laboratory for Study of the Earth's Interior and Geofluids, Institute of Geochemistry, Chinese Academy of Sciences, Guiyang, Guizhou 550002, China

^b Department of Geology and Geophysics, Yale University, New Haven, CT 06520, USA

ARTICLE INFO

Article history:

Received 9 February 2009

Received in revised form 5 August 2009

Accepted 9 August 2009

Available online 4 September 2009

Editor: L. Stixrude

Keywords:

electrical conductivity

wadsleyite

oxygen fugacity

frequency

water

ABSTRACT

The electrical conductivity of wadsleyite aggregates has been determined under the broad range of thermodynamic conditions using the impedance spectroscopy for a frequency range of 10^{-2} to 10^6 Hz. Two branches are observed in the complex impedance, one (at high frequency range) showing a half circle originated at Z' (real part of impedance) = Z'' (imaginary part of impedance) = 0 in the $Z'-Z''$ plot, and another branch in the low frequency range. The results from high frequency semi-circles correspond to the electric properties of a sample, whereas the results from a low frequency branch correspond to the electrode effects. From the analysis of the results from the semi-circles, we have identified two distinct mechanisms of electrical conduction having different activation enthalpies and different sensitivity to oxygen fugacity and water content. One mechanism dominating at water-poor condition has a high activation enthalpy (~ 147 kJ/mol) and the conductivity increases with oxygen fugacity. We suggest that electrical conduction in this regime is due to charge transfer involving ferric iron ("polaron" conduction). Under water-rich conditions, electrical conductivity increases with water content but decreases with oxygen fugacity, and the activation enthalpy is smaller (~ 88 kJ/mol). We infer that electrical conduction in this regime is due to protons. The activation enthalpy in this regime is insensitive to water content and the conductivity is proportional to water content, C_w , as $\sigma \propto C_w^r$ with $r \sim 0.72$. The value of r is smaller than one suggests that minority defects such as H_M' or H^\bullet are responsible for electrical conduction. Our results show that a completely dry transition zone is incompatible with most of the geophysical observations on the mantle transition zone, and some water (~ 0.1 – 0.3 wt.% in the Pacific) is required to explain the observed electrical conductivity.

© 2009 Elsevier B.V. All rights reserved.

1. Introduction

Electrical conductivity of minerals may be enhanced by the dissolution of water (hydrogen) (Karato, 1990). If this hypothesis is true, then we can in principle infer the water content in Earth's interior by comparing geophysically inferred conductivity profiles with laboratory data on the relation between electrical conductivity and water content (Karato, 2006). A few experimental studies have been conducted to test this hypothesis (wadsleyite: (Huang et al., 2005; Yoshino et al., 2008a; Romano et al., 2009)), olivine: (Wang et al., 2006; Yoshino et al., 2006)). However, there are complications in the experimental measurements of electrical conductivity and there have been some discrepancies among different studies on this topic. (Huang et al., 2005) found a large influence of water on the electrical conductivity of wadsleyite and estimated the water content in the transition zone is ~ 0.1 – 0.2 wt.%. In contrast, Yoshino et al. (2008a) and Manthilake et al. (2009) presented results somewhat different from those by Huang et al. (2005) and argued that the transition zone (in the

Pacific) is "dry" (water-free). Yoshino et al. (2008a) and Manthilake et al. (2009) determined the electrical conductivity of wadsleyite under broader temperature and water content conditions than Huang et al. (2005) but using a different experimental method. Karato and Dai (2009) provided some discussions on the influence of different methods of conductivity measurements (see also (Yoshino and Katsura, 2009a)). Also, the influence of another important parameter, namely oxygen fugacity was not determined in these previous studies.

Therefore the main purpose of this study is to revisit the issue of influence of water on the electrical conductivity of wadsleyite through a more extensive study than (Huang et al., 2005) to establish the relationship between physico-chemical variables and electrical conductivity on the more solid basis and to explore the causes for differences in the results from two research groups. We have expanded our previous study (Huang et al., 2005) in three respects: (i) we now add the results of conductivity measurements for a nearly water-free sample, (ii) the complex impedance was measured to lower frequencies (to 0.01 Hz) to investigate the causes for the discrepancy between the two sets of results, (iii) the influence of oxygen fugacity was determined to provide a firmer constraint on the mechanisms of electrical conductivity and (iv) the temperature and water content sensitivities were determined under a broader range of conditions.

* Corresponding author. Tel.: +1 203 432 3147; fax: +1 203 432 3134.
E-mail address: shun-ichiro.karato@yale.edu (S. Karato).

2. Experimental procedures

2.1. Sample preparation

Wadsleyite samples were synthesized from San Carlos olivine by phase transformation at 16 GPa and 1573 K. About 1.5 wt.% of orthopyroxene was added to buffer the oxide activity. Powder samples of olivine and orthopyroxene mixture were put into a metal capsule (Mo, Ni and Re were used to test the influence of different oxygen fugacity). Both synthesis and conductivity measurements were made using the same oxygen fugacity buffer. Our previous experience showed that under these conditions, the oxidation conditions of samples are well buffered by the metal and metal oxide reactions (e.g., (Nishihara et al., 2006, 2008)) and the presence of metal oxide such as ReO_2 was confirmed in most cases although the detection of metal oxide was difficult in cases where the volume of metal oxide is small. Each synthetic sample was examined by the micro-Raman spectroscopy to ensure that they are indeed wadsleyite. We obtained dense polycrystalline wadsleyite (with a small amount of majorite garnet) with a range of water content.

Water content of the samples was controlled in two different ways. In some synthesis runs, no water was added to a sample capsule, but some water was dissolved in the samples presumably from adsorbed water in the cell assembly. In other cases where a larger amount of water is to be dissolved, we add a talc–brucite mixture as described by Huang et al. (2005). The synthesis of a truly “dry” wadsleyite sample is not straightforward as discussed by Huang et al. (2005) and Nishihara et al. (2006). We used carefully dried parts and starting powder sample was inserted in an Au–Pd capsule with another metal foil to control the oxygen fugacity. As we will show, even the best case we had so far, a sample still had some water (less than 8 ppm H/Si), but that was the driest sample of wadsleyite that we ever had.

2.2. Sample characterization

Both before and after each electrical conductivity measurement, the grain-size was measured by an intercept method using a scanning electron microscope. The grain-size is nearly homogeneous in all samples within an error of measurements (~20%). There was no detectable change in grain-size during conductivity measurements. However, the influence of grain-size on electrical conductivity was not investigated systematically in this study. Similarly the previous studies on olivine aggregates by Huang et al. (2005) and Roberts and Tyburczy (1991) did not find a large effect of grain-size. Therefore, we consider that we may ignore the grain-size effect here.

Fourier-transformed infrared (FT-IR) spectroscopy was used to determine the water content. For all samples, FT-IR measurements were made both before and after each conductivity measurements for the wave-number range of 1000 to 4000 cm^{-1} . FT-IR absorption spectra of most of the samples are shown in Fig. 1. The doubly polished samples with a thickness of less than 60 μm were prepared for the FT-IR analysis. The FT-IR absorption spectra of samples were taken using an un-polarized IR beam with a mid-IR light source, a KI beam splitter and an MCT detector. One hundred twenty eight times scans were accumulated for each spectrum. Apertures of $100 \times 100 \mu\text{m}$ were applied for the measurements of selected sample areas.

The water (hydrogen) content of a sample was calculated from the absorption spectrum from 3000 to 3750 cm^{-1} wave-number range using the relation proposed by Paterson (1982),

$$C_w = \frac{B_i}{150\xi} \int \frac{K(\nu)}{(3780 - \nu)} d\nu \quad (1)$$

where C_w is the molar concentration of hydroxyl ($\text{H}/10^6 \text{ Si}$), B_i is the density coefficient ($4.08 \times 10^4 \text{ cm H}/10^6 \text{ Si}$), ξ is the orientation factor

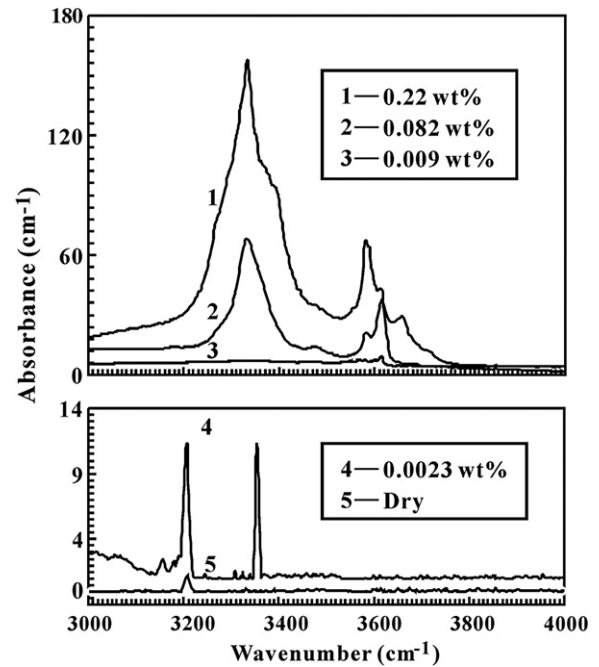


Fig. 1. FTIR spectra of wadsleyite for the wave-number range of 3000–4000 cm^{-1} .

($1/3$), and $K(\nu)$ is the absorption coefficient in cm^{-1} at the wave-number ν (cm^{-1}). The raw FT-IR spectra from most of wadsleyite samples have well-defined “base-line” and therefore there are no major issues of base-line correction that is an important source for uncertainties in olivine (e.g., (Kohlstedt et al., 1996)). Also Koga et al. (2003) showed that there are no major differences in the measured water content from FT-IR (using the Paterson calibration) and SIMS measurements for wadsleyite. Consequently, the water content estimate for wadsleyite has relatively small errors, on the order of ~10%. However, when the total water content becomes small, the relative errors become larger. For example, for the driest sample, our measurement showed ~8 ppm H/Si, but this is close to the detectability limit and errors are as large as $\pm 50\%$ in this case. We also note that the peak frequency of absorption for this sample is different from the peak frequencies of other water-rich samples indicating a different hydrogen-related species is involved in this sample (see (Nishihara et al., 2008)). Therefore the results from this sample cannot be compared with the results from other water-rich samples directly.

As we will show later, a sample with the smallest water content showed different behavior in electrical conductivity than samples with higher water content. We will call that sample “dry” wadsleyite and others as “wet” wadsleyite. Water content was determined both before and after the electrical conductivity measurements of hydrous sample, and the water loss is not more than 15%.

2.3. Conductivity measurements

The experimental sample assembly is shown in Fig. 2. Pressure was generated by a 1000-ton Kawai-type hydraulic press using eight cubic tungsten carbide anvils (Spec: $26 \times 26 \times 26 \text{ mm}^3$) with an 8 mm truncated carbide edge length. Pressure calibrations were made using the phase transitions of coesite and stishovite ((Zhang et al., 1996), 9.5 GPa and 1573 K), as well as forsterite and wadsleyite ((Morishima et al., 2004), 14.5 GPa and 1573 K). A Cr_2O_3 -doped (5%) semi-sintered octahedral MgO was used as a pressure medium. In order to avoid the influence of adsorbed water on the measurement of electrical conductivity, MgO was dried at 1273 K in air prior to sample assemblage. In order to control the oxygen fugacity of the sample

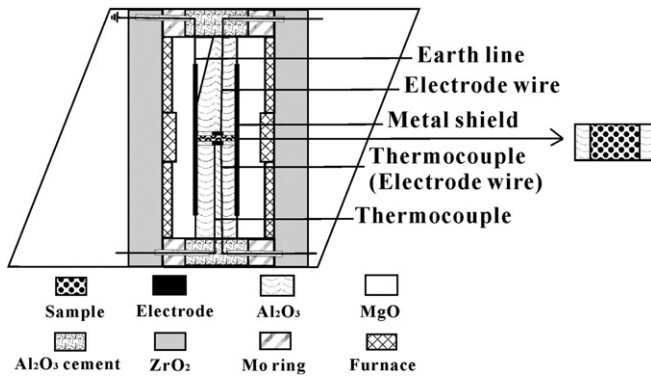


Fig. 2. Experimental setup for electrical conductivity measurements at high pressure and temperature.

chamber and reduce the leakage currents, a corresponding metal foil shielding was placed between a sample and an MgO insulation tube. A disk-shaped sample ($\text{\O}1.6 \times 0.4$ mm) was placed between two electrodes that were surrounded by alumina rings. The metal of electrode and the shielding foil are made of the same material as the capsule used for the synthesis of the sample. The temperature was measured by a $\text{W}_{26\%}\text{Re}-\text{W}_{5\%}\text{Re}$ thermocouple that was placed on the surface of sample and used as one of the electrodes (a thermocouple is connected to an electrode but does not directly touch the sample and therefore a thermocouple will not directly affect the oxygen fugacity of a sample). The relative experimental errors of the temperature and pressure gradient were estimated to be ~ 10 K and ~ 0.5 GPa, respectively. The errors in electrical conductivity measurement through the impedance fitting were estimated to be less than 5%.

The pressure was first raised at the rate of ~ 2.5 GPa/h to a designated value. After the pressure is set to the desired value, temperature was raised at the rate of ~ 100 K/min to the preset value and the impedance spectroscopy measurements were made at various temperatures. After the temperature reached to an each value, the ZPlot program of a Solartron-1260 Impedance/Gain-Phase analyzer was run to determine the complex impedance for the frequency range of $f = 10^{-2}$ – 10^6 Hz. The impedance semi-circle arc of high frequency branch (from 10^6 Hz to $\sim 10^2$ – 10^3 Hz) was fitted by virtue of an equivalent circuit of the ZView program that was made up of a resistance connected in parallel with a capacitor. From the fitting of the semi-circle to this model, we determine the conductivity of a sample.

The frequency range used in this study is broader than that used by Huang et al. (2005). This “impedance spectroscopy” approach is critical when there is a mechanism of charge built-up. When electric charge is built-up somewhere in the sample (or at the electrode), electric response of a sample to applied voltage includes capacitance as well as resistance. In order to make correction for the capacitance effect, it is necessary to analyze the data from a broad frequency range. However, in some studies (e.g., (Katsura et al., 1998; Yoshino et al., 2006; Yoshino et al., 2008b; Yoshino and Katsura, 2009b)), they only adopt one frequency (0.01 Hz, in most case) to calculate the electrical conductivity of a sample. Therefore in order to see the consequence of different methods of determining the conductivity, we have also calculated the conductivity from single frequency (0.01 Hz). Typical results of impedance spectroscopy are shown in Fig. 3. We observed two branches for each set of measurement, which we call a high frequency semi-circle and a low frequency tail. The frequency at which a transition from semi-circle to tail occurs increases with increasing temperature and is higher for a sample with higher water content. It is about 200 Hz at 873 K and 500 Hz at 1273 K for “dry” sample, whereas it is 320 Hz at 873 K and 800 Hz at 1273 K for a sample with 0.22 wt.% water.

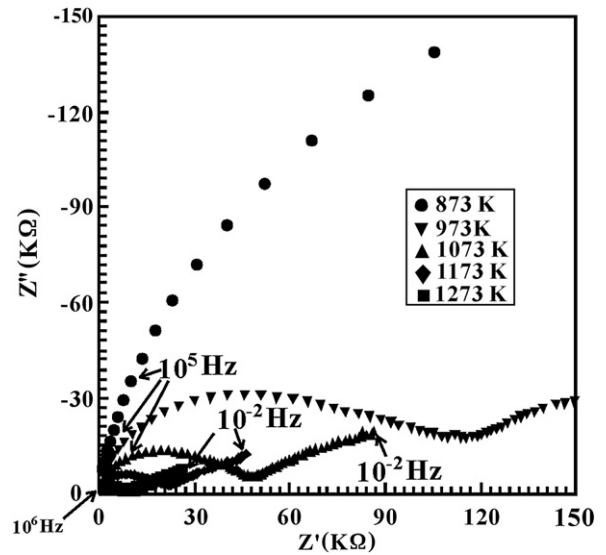


Fig. 3. Z'' vs. Z' plot of complex impedance of hydrous wadsleyite from 10^{-2} – 10^6 Hz (right to left), obtained under conditions of 15 GPa, 873–1273 K and 0.22 wt.% water content. Z' and Z'' are the real and imaginary part of complex impedance respectively.

The presence of two branches in the impedance spectroscopy implies the presence of two processes of charge transfer and/or blocking. The first semi-circle starting from the origin ($Z' = Z'' = 0$) corresponds to a parallel combination of a resistor and a capacitor, and the second branch (“tail”) at low frequencies corresponds to some blocking effects of electric current either at electrodes or at grain-boundaries (or both) (Macdonald et al., 1982; Cemič, 1996). Therefore we determined the conductivity from the fitting of the first semi-circle to equivalent circuit that is made of a parallel combination of resistor and capacitor.

Fig. 4 shows the results for the resistance measurements for a temperature cycling. We found no large hysteresis suggesting that the conductivity that we measure represents nearly equilibrium value for a given physical and chemical conditions at each measurement. This is also consistent with the observation that no appreciable water loss is detected in our study.

In order to make sure that the results are not affected by the leak current through the sample and the shield separated by an Al_2O_3 ring, we measured the “background resistivity”. In this background test, a sample is replaced with an Al_2O_3 disc with the dimension of

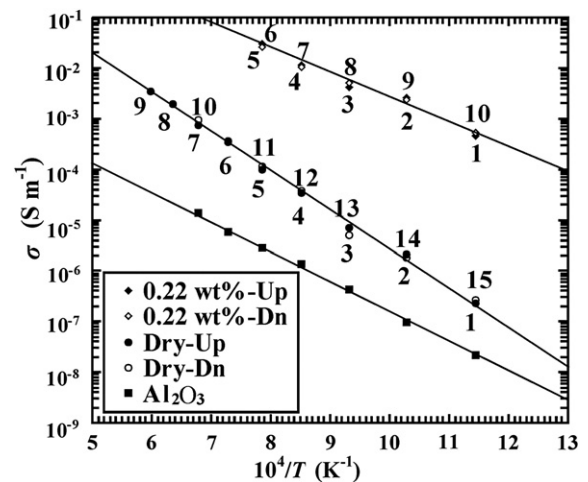


Fig. 4. A diagram showing the influence of measurement path on electrical conductivity for wadsleyite. Shown together are the conductivity of alumina used as an insulating material between a sample and the shield.

$\phi 1.6 \times 0.4$ mm and the resistance of this material was measured at $P = 15$ GPa and $T = 873$ – 1273 K. We found that the resistance of an Al_2O_3 disc is $\sim 10^2$ times higher than anhydrous samples and more than $\sim 10^5$ times higher than for hydrous samples. We conclude that the influence of leak current is minimal under our experimental conditions.

3. Results

The run conditions are summarized in Table 1. The electrical conductivity of the samples was calculated using the following equation, $\sigma = \frac{L/S}{R} = \frac{L}{SR}$ where L is the sample thickness and S is the cross section area of the electrode. The results of conductivity measurements for samples for Mo–MoO₂ buffer are shown in Fig. 5. It is seen that the electrical conductivity increases with temperature. The relationship between electrical conductivity and temperature approximately follows the Arrhenius relation, $\sigma \propto \exp\left(-\frac{H^*}{RT}\right)$, where H^* is the activation enthalpy. However, the activation enthalpy is different between “dry” and water-rich samples: $H^* = 147 \pm 3$ kJ/mol for a dry sample whereas $H^* = 88 \pm 10$ kJ/mol for water-rich samples. It should be noted that we also determined activation enthalpies for “wet” samples with different water content individually. The results are shown in Table 2. However, we observed that the activation enthalpy in “wet” samples is nearly independent of water content. A sample with an intermediate value of water content (K865) shows a mixed trend: at low temperatures, the slope in this plot follows that of water-rich samples, but the slope becomes close to that of a dry sample at higher temperatures. This suggests that there are two independent mechanisms of electrical conduction in these samples. Note that the activation enthalpy for water-rich sample does not depend on the water content in the water content range explored in our study.

Fig. 6 shows the relation between water content and electrical conductivity in water-rich samples (for the Mo–MoO₂ buffer). The electrical conductivity increases with water content following $\sigma \propto C_W^r$ with $r = 0.72 \pm 0.08$ that is consistent with the results by Huang et al. (2005) and is similar to the results for olivine (Wang et al., 2006) and pyrope garnet (Dai and Karato, 2009).

In order to obtain additional constraints on the mechanisms of electrical conductivity in two regimes (“dry” and “wet” (water-rich) regimes), we have determined the influence of oxygen fugacity on electrical conductivity using three different oxygen fugacity buffers. The results are shown in Fig. 7. The electrical conductivity increases with increasing oxygen fugacity for a “dry” sample, whereas the electrical conductivity decreases with oxygen fugacity for water-rich samples. If we use the relation $\sigma \propto f_{\text{O}_2}^q$, $q = 0.050 \pm 0.009$ for “dry” sample and $q = -0.058 \pm 0.004$ for “wet” sample.

The differences in activation enthalpy and in the dependence on oxygen fugacity for two types of samples (“dry” and “wet” (water-rich)) clearly indicate that the mechanism of electrical conductivity is

Table 1
Summary of runs.

Run no.	P (GPa)	T (K)	Water content (H/10 ⁶ Si)		Oxygen buffer	Grain size (μm)
			Before experiment	After experiment		
K736	15	873–1273	1400	1280	Mo–MoO ₂	7
K743	15	873–1273	34,000	32,000	Mo–MoO ₂	5
K787	15	873–1673	<8	<9	Mo–MoO ₂	9
K792	15	873–1273	13,000	12,000	Mo–MoO ₂	5
K814	15	873–1273	12,000	11,000	Ni–NiO	4
K819	15	873–1273	<5	<7	Re–ReO ₂	3
K820	15	873–1273	<7	<8	Ni–NiO	7
K826	15	873–1273	18,000	16,000	Re–ReO ₂	6
K865	15	873–1473	360	350	Mo–MoO ₂	4

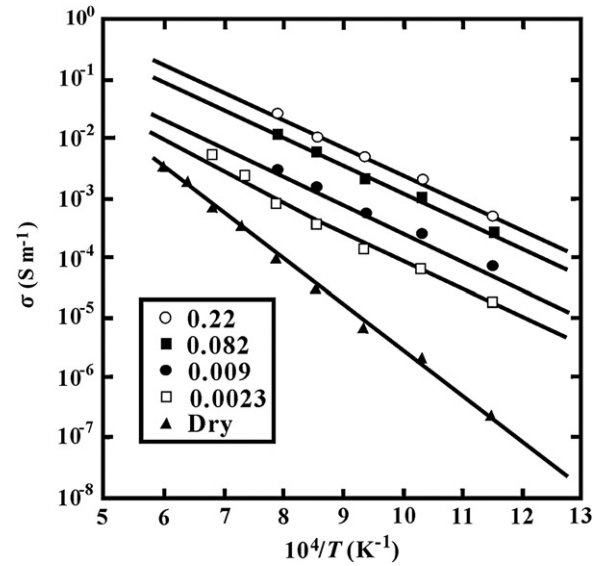


Fig. 5. Electrical conductivity of wadsleyite versus inverse temperature relationship at $P = 15$ GPa and 873–1673 K for different water contents.

different under these two conditions. Consequently, we use the following formula to analyze the data,

$$\sigma = \sigma_1 + \sigma_2 \quad (2)$$

where σ_1 is the electrical conductivity of a “dry” sample and σ_2 is the electrical conductivity of “wet” (water-rich) samples. For each mechanism, we use the following formula,

$$\sigma = A \cdot C_W^r \cdot f_{\text{O}_2}^q \cdot \exp\left(-\frac{H^*}{RT}\right) \quad (3)$$

where A , r , q are the constants, C_W is the water content, H^* is the activation enthalpy, R is the gas constant and T is temperature. The parameters for each mechanism are summarized in Table 2. The fitted parameter values for the electrical conductivity of “wet” and “dry” wadsleyite are listed in Table 2.

Table 2
Parameter values for the electrical conductivity of wadsleyite.

Samples	Log_{10} (A(S/m))	r	H^* (kJ mol ⁻¹)
Wet (all data)	2.5 ± 0.5	0.72 ± 0.08	88 ± 10
0.22 wt.%	2.5 ± 0.2	0.72	88 ± 3
0.082 wt.%	2.4 ± 0.1	0.72	87 ± 3
0.009 wt.%	2.5 ± 0.2	0.72	86 ± 3
0.0023 wt.%	2.6 ± 0.3	0.72	91 ± 6
Dry	2.1 ± 0.1	0	147 ± 3

The relation $\sigma = A \cdot C_W^r \cdot \exp\left(-\frac{H^*}{RT}\right)$ is used. For individual fitting for each water content, the corresponding value of C_W^r (with $r = 0.72$) was used (the assumed value of r does not influence the estimated H^* and therefore the error in r is not included in the estimate of A and H^* for individual fitting). The reported errors are the one standardized deviation, and include the contribution of errors in individual measurements (errors in water content, temperature and electrical conductivity). The errors and the value of H^* for 0.0023 wt.% sample are larger than those of other “wet” samples due to the appreciable contributions of two mechanisms of conduction under these conditions leading to a curvature in the log(conductivity) versus $1/T$ (temperature) plot (see Fig. 5). Conductivity is assumed to be independent of grain-size (as shown by (Huang et al., 2005)).

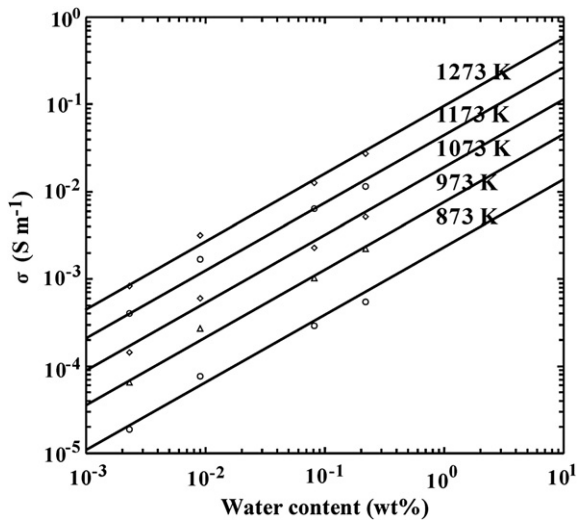


Fig. 6. Electrical conductivity versus water content relation for “wet” (water-rich) wadsleyite under conditions of 15 GPa and 873–1273 K.

4. Discussion

4.1. Conduction mechanisms

The observed different activation enthalpy and different dependence on oxygen fugacity for “dry” and “wet” (water-rich) samples are strong evidence for the operation of different mechanisms of electrical conduction in these two types of samples. In particular, the dependence of conductivity on oxygen fugacity and water fugacity (the exponent r and q in Eq. (3)) provide strong constraints on the nature of point defects involved in electrical conductivity (see Chapter 10 of Karato (2008) for details). The observed positive exponent for oxygen fugacity for a “dry” sample is consistent with the charge transfer by ferric iron (Fe) with charge neutrality conditions either $[Fe_M^\bullet] = 2[V_M'']$ ($q = 1/6$) or $[Fe_M^\bullet] = [H_M']$ ($q = 1/8$) (e.g., (Karato, 2008)). The activation enthalpy of 147 kJ/mol is similar to the values observed in dry olivine (154 kJ/mol) and pyrope (141 kJ/mol, (Dai and Karato, 2009)), and in case of olivine, there is a strong evidence for ferric iron-related conduction mechanism based on the oxygen fugacity dependence as well as the results of thermo-electric power measurements (Schock et al., 1989). However, the value of oxygen fugacity exponent, q (~ 0.050), is lower than those predicted by simple

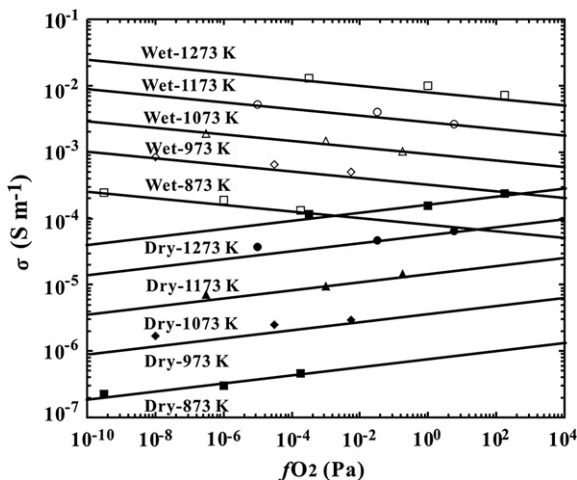


Fig. 7. Electrical conductivity of “dry” and “wet” wadsleyite versus inverse three oxygen buffers (e.g. Mo–MoO₂, Ni–NiO and Re–ReO₂) under the conditions of 15 GPa and 873–1273 K. The “wet” data are normalized to 0.074 wt.% water content.

models. It is possible that the oxygen fugacity range explored spans these charge neutrality conditions as well as other conditions such as $[e'] = [Fe_M^\bullet]$ where $[Fe_M^\bullet]$ is independent of oxygen fugacity. An alternative possibility is imperfect equilibrium with respect to the oxygen fugacity buffer, although we consider this is unlikely because of the lack of appreciable hysteresis in our conductivity measurements.

The results for “wet” (water-rich) samples are similar to those by Huang et al. (2005), but we have more robust results on the activation enthalpy and water content dependence, and we also have additional data on the dependence of conductivity on oxygen fugacity. First, for “wet” samples, the oxygen fugacity exponent, r , is negative. This is consistent with conductivity mechanisms involving protons. The observed results showing the value of r (0.72) of less than one means that the dominant hydrogen-related defect, $(2H)_M^\times$, is not the main charge carrier. Instead, some ionized defects such as H_M' with the charge neutrality condition of $[Fe_M^\bullet] = 2[V_M'']$ (this model predicts $r = 1/2$ and $q = -1/12$) or H^\bullet with the charge neutrality condition of $[Fe_M^\bullet] = [H']$ ($r = 3/4$ and $q = -1/8$) is a plausible model (Karato, 2008). The presence of such minority defects in wadsleyite is documented by Nishihara et al. (2008). This means that the minority defects such as H^\bullet or H_M' has higher mobility than the majority defect, $(2H)_M^\times$. Again, however, the absolute value of q ($= -0.058$) is less than these model predictions, suggesting that the experimental conditions may span more than one charge neutrality conditions or chemical equilibrium was only partial.

4.2. A comparison to previous studies

The present results are in good agreement with those by Huang et al. (2005), although the parameter range explored is much broader in the present study than that in Huang et al. (2005). For example, we have determined the temperature dependence of conductivity under a broader range of conditions, and new results on the influence of oxygen fugacity were obtained.

However, our results are not consistent with those by Yoshino et al. (2008a) and Manthilake et al. (2009). As discussed in detail by Karato and Dai (2009), most of the differences between our results and those by Yoshino et al. (2008a) and Manthilake et al. (2009) are due to the difference in the method of conductivity measurements (see also Romano et al. (2009)) and the difference in water content in “dry” samples. Essentially, the use of one (or two) low frequency to determine electrical conductivity results in a systematic bias for the determined conductivity due to the influence of charge blocking at electrodes. This influence is greater for samples with higher water contents. This point is shown in Fig. 8. It is seen that the difference in results from one low frequency measurements and impedance spectroscopy is larger for samples with larger water content. Also, the difference is larger at higher temperatures (under high water content conditions). We can largely reproduce Yoshino et al.’s results (Yoshino et al., 2008a) from our data if we use one frequency (0.01 Hz). Consequently, we consider that the most of the differences are due to the differences in the method of conductivity measurements.

The above analysis also implies that the reported water content dependence of activation enthalpy by Yoshino et al. (2008a) may be an experimental artifact. Both in Huang et al. (2005) and this study, we show that the activation enthalpy under water-rich conditions is insensitive to water content. As we discussed in detail before (see also (Karato and Dai, 2009)), one fundamental problem of Yoshino et al.’s. (2008a) approach is the use of a single low frequency to determine the conductivity that gives rise to a systematic bias on the inferred conductivity. This difference becomes larger at higher water content and higher temperature (in the water-rich regime), and consequently will result in the biased estimates of activation enthalpy. To evaluate the magnitude of this effect, we have calculated the activation enthalpy using our method as well as Yoshino et al.’s. (2008a) method. The results are compared in Fig. 9. It is seen that when we use Yoshino

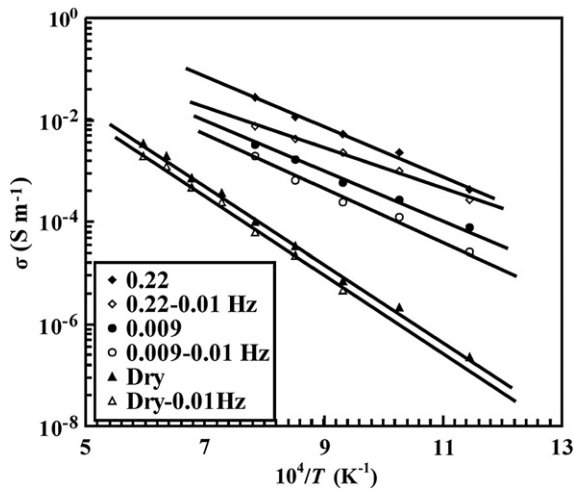


Fig. 8. Influence of method of calculation of electrical conductivity. The results from impedance spectroscopy analysis from the semi-circle fit are compared with the results based on single frequency (0.01 Hz) fit. Results for “wet” (0.22 and 0.009 wt.%) and “dry” samples are shown (at 15 GPa, 873–1673 K).

et al.’s method, we reproduce water content-dependent activation enthalpy that they reported, but the activation enthalpy is insensitive to water content, if the impedance spectroscopy technique is used. It is also noted that a sample with a small water content (K865) shows the influence of both protons (at low temperatures) and polarons (at high temperatures). The composite conductivity equation with parameters shown in Table 2 reproduce our results as shown in Fig. 5. Yoshino and Katsura (2009a) claimed that our data are internally inconsistent because the results from low water content samples (K865 and K787) are not compatible with other data with higher water contents. The above analysis shows that their claim is invalid because of their incorrect interpretation of results FT-IR study of water content and speciation.

We also note that Yoshino et al. (2008a) and Manthilake et al. (2009) measured electrical conductivity of “wet” samples at lower temperatures than most of our measurements. Consequently, conductivity mechanisms operating under their experimental con-

ditions might be different from those in our “wet” samples and this is a possible additional factor that may cause the difference in the results. In any case, either due to the artifact cause by the use of inappropriate method or by the use of the low temperatures (for “wet” samples), we conclude that the results by Yoshino et al. (2008a) and Manthilake et al. (2009) on “wet” wadsleyite cannot be applied to Earth’s interior.

4.3. Geophysical implications

The present study has provided additional data on the electrical conductivity of wadsleyite for a broad range of thermo-chemical conditions that forms a basis for estimating water content in the transition zone. Given a much lower solubility of hydrogen in garnet (Katayama et al., 2003) than that in wadsleyite (Kohlstedt et al., 1996), we may model the upper transition zone (410–520 km) as a mixture of highly conductive wadsleyite and less conductive majorite garnet. Because the more conductive component, wadsleyite, is volumetrically dominant, we can assume that wadsleyite forms a connected network. In such a case, geophysical estimates from a model corresponding to the upper bound (e.g., (McLachlan et al., 1990)) in the upper portion of the transition zone ranging from $\sigma = \beta \cdot \sigma_{\text{wad}}(T, C_w)$ with $\beta \approx 0.6$ to $\sigma_{\text{wad}}(T, C_w) = \sigma_1(T) + \sigma_2(T, C_w)$ that is given by the present results (we assumed 60% of wadsleyite and 40% of majorite).

Fig. 10 shows the T (temperature)– C_w (water content) trade off for a range of values of electrical conductivity of the upper transition zone. Geophysical estimates of electrical conductivity in the (upper) transition vary from one region to another but ranges from $\sim 10^{-2}$ S/m to ~ 1 S/m, most representative value being $\sim 10^{-1}$ S/m (e.g., (Utada et al., 2003; Tarits et al., 2004; Utada et al., 2005; Ichiki et al., 2006; Toffelmier and Tyburczy, 2007)). Under these conditions proton contributions are more important than polaron contributions and therefore one can infer water (proton) contents from the observed electrical conductivity. If the transition zone had a water content similar to the asthenosphere ($\sim 10^{-2}$ wt.%; (Hirschmann, 2006)), then in order to explain a typical conductivity of 10^{-1} S/m, one would need a temperature of ~ 2400 K, which is unacceptably high. For the representative temperature of $T \sim 1700$ – 1800 K, the water content of on the order of 10^{-1} wt.% can explain the electrical conductivity of $\sim 10^{-1}$ S/m. In order to obtain more

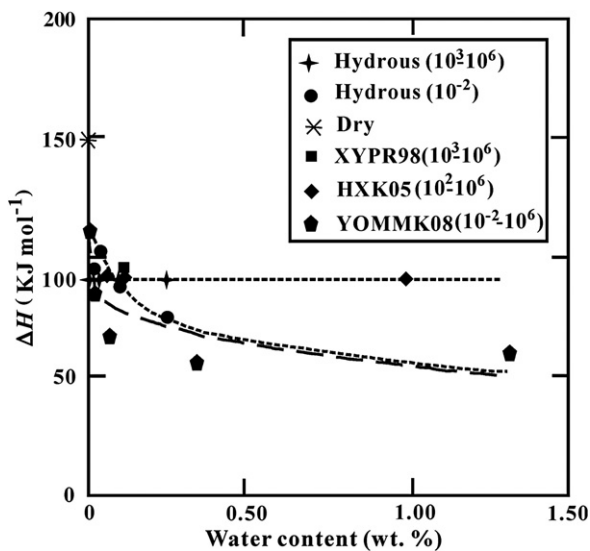


Fig. 9. The relationship between the activation enthalpy and water content for wadsleyite. Present results and those by Huang et al. (2005) show no dependence of activation enthalpy on water content, whereas if a single frequency was used, dependence of activation enthalpy on water content is seen due to the systematic bias caused by the charge build-up at electrode as seen in Fig. 8.

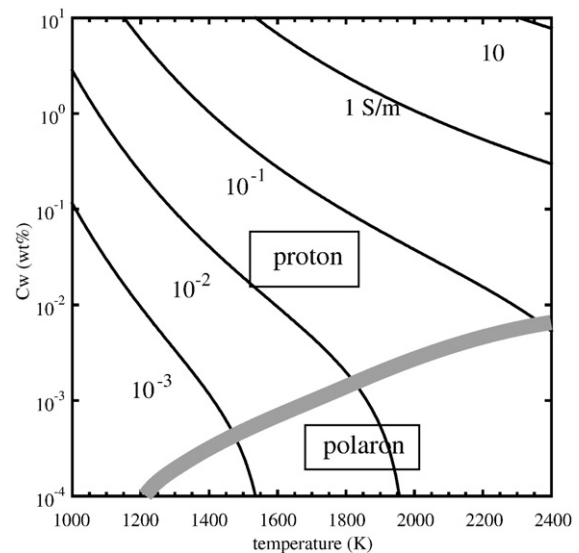


Fig. 10. Temperature (T)–water content (C_w) relationship corresponding to various conductivity values. The oxygen fugacity corresponding to Mo–MoO₂ buffer is assumed. A grey thick curve shows a boundary between proton-dominated regime and polaron-dominated regime. Most of conductivity data for Earth’s transition zone fall into the proton-dominated regime.

robust estimates of water content, one needs to obtain better experimental data electrical conductivity of majorite garnet and independent estimates of temperature.

Acknowledgements

We thank Mainak Mookherjee, Zhicheng Jing and Zhenjing Jiang for the technical assistance. This research is financially supported by the NSF of China (Grant No. 40704010) and the NSF of the United States (Grant No. 0608579).

References

- Cemič, L., 1996. Impedance spectroscopy and defect chemistry of fayalite. *Phys. Chem. Miner.* 23, 186–192.
- Dai, L., Karato, S., 2009. Electrical conductivity of pyrope-rich garnet at high temperature and pressure. *Phys. Earth Planet. Inter.* 176, 83–88.
- Hirschmann, M.M., 2006. Water, melting, and the deep Earth H₂O cycle. *Annu. Rev. Earth Planet. Sci.* 34, 629–653.
- Huang, X., et al., 2005. Water content of the mantle transition zone from the electrical conductivity of wadsleyite and ringwoodite. *Nature* 434, 746–749.
- Ichiki, M., et al., 2006. Water content and geotherm in the upper mantle above the stagnant slab: interpretation of electrical conductivity and seismic P-wave velocity models. *Phys. Earth Planet. Inter.* 155, 1–15.
- Karato, S., 1990. The role of hydrogen in the electrical conductivity of the upper mantle. *Nature* 347, 272–273.
- Karato, S., 2006. Remote sensing of hydrogen in Earth's mantle. In: Keppler, H., Smyth, J.R. (Eds.), *Water in Nominally Anhydrous Minerals*. In Mineralogical Society of America, Washington DC, pp. 343–375.
- Karato, S., 2008. *Deformation of earth materials: introduction to the rheology of the solid earth*. Cambridge University Press, Cambridge. 463 pp.
- Karato, S., Dai, L., 2009. Comments on “Electrical conductivity of wadsleyite as a function of temperature and water content” by Manthilake et al. *Phys. Earth Planet. Inter.* 174, 19–21.
- Katayama, I., et al., 2003. Water solubility in majorite garnet in subducting oceanic crust. *Geophys. Res. Lett.* 30. doi:10.1029/2003GL018127.
- Katsura, T., et al., 1998. Electrical conductivity of silicate perovskite at lower-mantle conditions. *Nature* 395, 493–495.
- Koga, K., et al., 2003. Hydrogen concentration and analyses using SIMS and FTIR: comparison and calibration for nominally anhydrous minerals. *Geochem. Geophys. Geosyst.* 4. doi:10.1029/2002GC000378.
- Kohlstedt, D.L., et al., 1996. Solubility of water in the α , β and γ phases of (Mg,Fe)₂SiO₄. *Contrib. Mineral. Petrol.* 123, 345–357.
- Macdonald, J.R., et al., 1982. The applicability and power of complex nonlinear least squares for the analysis of impedance and admittance data. *J. Electroanal. Chem.* 131, 77–95.
- Manthilake, M.A.G.M., et al., 2009. Electrical conductivity of wadsleyite as a function of temperature and water content. *Phys. Earth Planet. Inter.* 174, 10–18.
- McLachlan, D.S., et al., 1990. Electrical resistivity of composite. *J. Am. Ceram. Soc.* 73, 2187–2203.
- Morishima, H., et al., 2004. The phase-boundary between alpha-Mg₂SiO₄ and beta-Mg₂SiO₄ determined by in-situ X-ray observation. *Science* 265, 1202–1203.
- Nishihara, Y., et al., 2006. Grain-growth kinetics in wadsleyite: effects of chemical environment. *Phys. Earth Planet. Inter.* 154, 30–43.
- Nishihara, Y., et al., 2008. Effects of chemical environments on the hydrogen-defects in wadsleyite. *Am. Mineral.* 93, 831–843.
- Paterson, M.S., 1982. The determination of hydroxyl by infrared absorption in quartz, silicate glass and similar materials. *Bull. Mineral.* 105, 20–29.
- Roberts, J., Tyburczy, J.A., 1991. Frequency dependent electrical properties of polycrystalline olivine compacts. *J. Geophys. Res.* 96, 16205–16222.
- Romano, C., et al., 2009. Electrical conductivity of hydrous wadsleyite. *Eur. J. Mineral.* 21, 615–622.
- Schock, R.N., et al., 1989. Electrical conduction in olivine. *J. Geophys. Res.* 94, 5829–5839.
- Tarits, P., et al., 2004. Water in the mantle: results from electrical conductivity beneath the French Alps. *Geophys. Res. Lett.* 31. doi:10.1029/2003GL019277.
- Toffelmier, D.A., Tyburczy, J.A., 2007. Electromagnetic detection of a 410-km-deep melt layer in the southwestern United States. *Nature* 447, 991–994.
- Utada, H., et al., 2003. A semi-global reference model for electrical conductivity in the mid-mantle beneath the north Pacific region. *Geophys. Res. Lett.* 30. doi:10.1029/2002GL016092.
- Utada, H., et al., 2005. Electrical conductivity in the transition zone beneath the North Pacific and its implications for the presence of water. *EOS, Transact. Am. Geophys. Union* 86, D141A–1260.
- Wang, D., et al., 2006. The effect of water on the electrical conductivity in olivine. *Nature* 443, 977–980.
- Yoshino, T., Katsura, T., 2009a. Reply to comments on “Electrical conductivity of wadsleyite as a function of temperature and water content” by Manthilake et al. *Phys. Earth Planet. Inter.* 174, 22–23.
- Yoshino, T., Katsura, T., 2009b. Effect of iron content on electrical conductivity of ringwoodite, with implications for electrical structure in the transition zone. *Phys. Earth Planet. Inter.* 174, 3–9.
- Yoshino, T., et al., 2006. Hydrous olivine unable to account for conductivity anomaly at the top of the asthenosphere. *Nature* 443, 974–976.
- Yoshino, T., et al., 2008a. Dry mantle transition zone inferred from the conductivity of wadsleyite and ringwoodite. *Nature* 451, 326–329.
- Yoshino, T., et al., 2008b. Electrical conductivity of majorite garnet and its implications for electrical structure in the mantle transition zone. *Phys. Earth Planet. Inter.* 170, 193–200.
- Zhang, J., et al., 1996. In situ X-ray observations of the coesite–stichovite transition: reversed phase boundary and kinetics. *Phys. Chem. Miner.* 23, 1–10.